Am J Cancer Res 2021;11(3):916-929
www.ajcr.us /ISSN:2156-6976/ajcr0121344

Original Article

Decreased NSG3 enhances PD-L1 expression by Erk1/2 pathway to promote pancreatic cancer progress

Xigang Xia[1,2,3*], Ran Li[3,4*], Peng Zhou[1,3], Zhixiang Xing[1,3], Chao Lu[1,3], Zhida Long[1,3], Feiyang Wang[3,5], Rui Wang[1,3]

[1]The Second Clinical Medical College, Jingzhou Central Hospital, Yangtze University, Jingzhou 434020, China; [2]Pancreatic Surgery, Zhongnan Hospital of Wuhan University, Wuhan 430022, China; [3]Sino-German Laboratory of Personalized Medicine for Pancreatic Cancer, Union Hospital, Tongji Medical College, Huazhong University of Science and Technology, Wuhan 430022, China; [4]Guizhou Medical University, University Town, Guian New District, Guizhou 550025, China; [5]Department of General Surgery, Shanghai General Hospital, Shanghai Jiao Tong University School of Medicine, Shanghai, China. [*]Equal contributors.

Received August 29, 2020; Accepted November 3, 2020; Epub March 1, 2021; Published March 15, 2021

Abstract: Inhibiting the functioning of PD-1/PD-L1 to activate human immune system and improve the prognosis of pancreatic cancer (PC) would provide a significant boost to handling the disease. One research found the expression level of NSG3 was reduced in pediatric pilocytic astrocytoma, so is PC and we found NSG3 could regulate the expression of PD-L1. So NSG3 could become a new target for enhancing the immune response to PC. The GEPIA website was employed to analyze the prognoses in PC patients with different NSG3 levels. Immunohistochemistry (IHC) analysis was applied to detect different levels of NSG3 in para-PC and PC tissues. Cell biological function tests (*in vitro*) were performed and a subcutaneous nude mice tumor model (*in vivo*) was established to verify the effect of NSG3 on PC. Immunoblotting and RT-qPCR were utilized to demonstrate the inhibiting effect of NSG3 on PD-L1 through regulating Erk1/2 phosphorylation. A subcutaneous C57BL/6 tumor mice model was established to assess the possibility of a synergistic effect of NSG3 expression and the use of an anti-PD-L1 antibody on PC. PC tissues had decreased NSG3 expression levels, which led to poor prognosis. Overexpressing NSG3 suppressed proliferation, invasion and migration capacities of PC cells. On the contrary, knocking-down NSG3 prompted PC malignancy whether *in vivo* or *in vitro*. Importantly, NSG3 prevented Erk1/2 phosphorylation to inhibit PD-L1 expression. Additionally, NSG3 and an immune checkpoint inhibitor anti-PD-1 antibody acted synergistically, which enhanced the efficacy of the inhibitor. NSG3 inhibited PD-L1 expression by suppressing Erk1/2 phosphorylation to improve the immune response to PC. NSG3 is, therefore, a potential new diagnostic and prognostic marker, particularly useful in immune checkpoint blockade therapy.

Keywords: NSG3, pancreatic cancer, PD-L1, anti-PD-1 antibody, Erk1/2 phosphorylation

Introduction

Pancreatic cancer (PC) has been recognized as one of the most deadly neoplasms [1, 2], with rapidly rising morbidity and mortality [3]. Because of locally advanced and systemic metastases in PC, the disease has a poor prognosis with only 8% of 5-year survival rate [4]. The main treatment option for PC is surgical resection plus postoperative adjuvant chemotherapy, but only about 10% of PC patients are diagnosed early and can, therefore, undergo a surgical resection [3]. Even among those diagnosed early, there is a poor chemotherapy response due to drug resistance [5]. Hence, there is an urgent need to explore a new treatment option that can improve the prognosis of PC patients.

Tumor immunotherapy, a burgeoning therapy method, kills tumor cells by activating the body's immune system [6]. In recent years, immune checkpoint inhibitors have become a focal point in tumor immunotherapy, particularly those that target the programmed cell death protein 1/programmed cell death-ligand 1 (PD-1/PD-L1) [7]. PD-L1 could lead to T cell dysfunction and failure by binding to external PD-1

on T cells [8]. CD80 (B7-1), another protein in immune cells, could also interact with PD-L1 to impede T cell activation [9]. Consequently, tumor cell invasiveness would increase, and a variety of cytokines, including TNF-α, IF-2, and IFN-γ, would be secreted as a result of the inactivation and depletion of CD8+ T cells [10]. Additionally, regulatory T cells (Treg, CD4+ Foxp3+) caused the highly immunosuppressive tumor environment through protecting the expression of PD-1 [11]. Therefore, inhibiting the function of PD-1/PD-L1 is of great significance to the enhancement of the immune response and improvement of the prognosis of pancreatic cancer.

Calcyon neuron-specific vesicular protein (CALY), also known as NSG3 or DRD1IP, is part of the triple NEEP21/P19/Calcyon gene family and can regulate vesicle transport events, including synaptic plasticity, neurodevelopment, and neurodegeneration [12-15]. As a nerve-enriched single transmembrane protein, NSG3 plays a crucial role in D1-like receptor Ca^{2+} signaling [16] and could also interact with the clathrin light chain (CLC) to promote clathrin assembly and clathrin-mediated endocytosis (CME) [12]. Interestingly, one study found that the individual clone deletion of NSG3 located on chromosome 10q26.3 causes reduced gene expression in pediatric pilocytic astrocytoma [17], indicating that NSG3 was related to the occurrence and development of tumors.

In this research, we found that pancreatic cancer cells had decreased expression of NSG3. We also determined that NSG3 exerted a major effect on inhibitingpancreatic cancer cells proliferation and metastasis. Furthermore, we revealed that NSG3 inhibited PD-L1 expression via reducing the phosphorylation levels of Erk1/2. In general, our research suggests that NSG3 is a potential enabler of immune checkpoint inhibitor to improve αPD-1 curative effects on pancreatic cancer.

Materials and methods

Cell lines and cell culture

We purchased three PC cell lines (PANC-1, BxPC-3 and SW1990) from the Chinese Academy of Science Cell Bank. All cell lines were cultured through Dulbecco's Modified Eagle Medium (DMEM) (Gibco, USA) with 10% fetal bovine serum (Gibco, USA), 100 U/ml penicillin, and 100 ug/ml streptomycin (Gibco, USA). All cell lines were incubated in a 37°C and 5% CO_2 incubator.

Cell transfection

All plasmids were constructed at Shanghai Genechem Co., LTD. A Lipofectamine 2000 reagent (Thermo Fisher Scientific) was utilized to transfect gene-specific small hairpin RNA (shControl and shNSG3) and Flag-tag plasmid (pcDNA3.1 and Flag-NSG3, human and mouse). The transfection system was completed with an Opti-MEM medium (Gibco, USA) to make up the full amount. The concentration of plasmid used was 3 ug/ml, and the total transfection system amounted to 1 ml. The Opti-MEM medium was replaced with the complete DMEM medium after transfecting 6 hours. Table S1 provided the information of shNSG3 sequences.

Lentivirus and the construction of stable cell lines

A lentiviral expression vector (hU6-MCS-CBh-gcGFP-IRES-puromycin) was used to infect and construct stable pancreatic cancer cells with knocked down or overexpressed NSG3. On day 0, 2×10^5 (per well) pancreatic cancer cells (PANC-1) were counted and plated in six-well plates with 1 mL complete medium. On day 1, an infectious solution was created using a complete medium, and it consisted of 1 ml of complete DMEM medium and 40 ul of Hitrans G reagent per well, according to the instructions (Shanghai Genechem Co., Ltd.). The old medium was then replaced with the infectious solution, and the quantity of virus required per well was calculated according to cell multiplicity of infection (MOI) and added to the infectious solution to infect cells. On day 2, after 16 hours of infection, the infectious solution was replaced with a conventional complete DMEM medium. Finally, puromycin was used to screen successfully infected cells after 72 hours of continuous culture.

Antibodies and reagents

The antibodies used included NSG3 (absin, abs138459, working concentration 1:1000), PD-L1 (Proteitech, 17952-1-AP, working con-

centration 1:1000), Erk1/2 (Cell Signaling Technology, 4695, working concentration 1:1000), pErk1/2-Thr202/Tyr204 (Cell Signaling Technology, 9101, working concentration 1:1000), and GAPDH (Proteitech, 10494-1-AP, working concentration 1:2000). The used inhibitor was AG126 (MedChemExpress, HY-108330, working concentration 25 uM).

Tissue microarray, immunohistochemistry, and pancreatic cancer specimens

We purchased the pancreatic cancer tissue microarray chips from Shanghai Outdo Biotech Co., LTD (Shanghai, China). We conducted immunohistochemical staining with an NSG3 antibody and a PD-L1 antibody. Immunohistochemical scoring was carried out independently by two pathologists not privy to the detailed information of the experimental procedure. The Staining index was defined as "staining intensity × percentage". Staining intensity scoring was accomplished per the following criteria: 1 = weak staining at 100 × magnification but little or no staining at 40 × magnification; 2 = medium staining at 40 × magnification; 3 = strong staining at 40 × magnification.

Clone formation and invasion assays

Six-well plates were used to carry out clone formation assays, with 1000 cells counted and seeded in each well. Media were replaced every three days. After two weeks, 4% paraformaldehyde was used to fix cell colonies for 30 minutes. Then crystal violet was used to stain the cell colonies for 20 minutes.

Cell invasion was assessed with Transwell chambers. The 24-well Corning Costar was inserted with 8-μm pores precoated with Matrigel (BD, USA, diluted 1:8) for 6 hours to assess the cell invasion in a 37°C and 5% CO_2 incubator. 500 ul (per well) of a DMEM medium with 30% FBS was added to the hole, and 200 ul (per well) of a serum-free DMEM medium comprising 1 × 10^5 cells was added to the upper chambers. After 24 hours of culture, 4% paraformaldehyde was used to fix the transwell chambers for 30 minutes and then a crystal violet solution was used to stain for another 30 minutes. Finally, a PBS buffer was used to cleanse the chambers, and photographs were taken with a microscope.

Western blotting

The total protein in cells and tumor tissues were lysed with a RIPA buffer containing 1% of protease inhibitors. Then the concentrations of the protein extracted were detected through a kit (Pierce Biotechnology, USA). The total protein lysis buffer was separated and analyzed with SDS-PAGE. Next, the protein was transferred to Polyvinylidene fluoride (PVDF) membranes (Pierce Biotechnology, USA) from the gel. Then 5% skim milk powder was employed to block PVDF membranes for 1 hour at room temperature and washing PVDF membranes. The membranes were incubated with the corresponding primary antibodies overnight at 4°C. Next, using 0.1% TBST buffer washed the membranes three times with 10 minutes each time. Then the membranes were incubated with secondary antibodies for another 1 hour on the shaker at room temperature. Finally, the ECL illuminating liquid (Thermo Fisher, USA) was used to expose the membranes under the illumination of X-rays.

Quantitative real-time polymerase chain reaction (RT-qPCR)

We utilized the Trizol reagent (Thermo Fisher Scientific, USA) to dissociate and extract total RNA. The extracted RNA was reverse transcribed to obtain cDNA based on the kit direction (PrimeScript™ RT reagent Kit). A RT-qPCR analysis was performed to amplify the cDNA utilizing a PCR kit (TB Green™ Fast qPCR Mix). The cycle index was normalized to GAPDH. Then 2-ΔCt method was employed to describe and illustrate multiple variations. Table S2 provided the information of forward and reverse primer sequences.

Nude mice xenograft transplantation model

BALB/c-nude mice (4-5 weeks old, 20 g) were from Vitalriver (Beijing, China). These animals were raised in a specific-pathogen-free (SPF) environment. We divided the mice into three groups randomly and equally. Each mouse was injected subcutaneously on the left-back with corresponding treated PANC-1 cells (5 × 10^6/mouse). The vernier caliper was used to measure the volume of the xenografts once every three days. Utilizing the formula (L × W2)/2 calculated the xenograft volumes. The mice were killed mercifully after feeding 30 days, and the xenografts were dissected and weighed.

Anti-PD-1 antibody treatment protocol

C57BL/6 mice (4-5 weeks old, 20 g) were from Vitalriver (Beijing, China). These animals were feeding in a SPF environment. Each mouse was injected subcutaneously at the left back with 5×10^6 PANC02 cells. All mice were randomly divided into four groups of five mice each after xenografts volume growed to 50 mm^3 Then the mice were injected 200 ug anti-PD-1 antibody (BioXcell, BE0146, USA) or IgG (BioXcell, BE0094, USA) intraperitoneally on days 0, 3, and 6.

After the natural death of the mice, the tumors were dissected to prepare single-cell suspensions. The following antibodies were utilized for staining cells: FITC conjugated CD4 antibody (Biolegend, 100,510, USA); PE-conjugated CD8 antibody (Biolegend, 100,708, USA); APC conjugated CD45 antibody (Biolegend, 103,112, USA); APC conjugated CD11b antibody (Biolegend, 101,212, USA); FITC conjugated Gr1 antibody (Biolegend, 108,406, USA). BD FACSCelesta (BD Biosciences, USA) was used to perform Flow cytometry and FlowJo was used to analyze the data.

Bioinformatics mining and analysis

The Gene Expression Profiling Interactive Analysis (GEPIA) website and Human Protein Atlas were employed to analyze the correlation between NSG3 expression and the survival rate of pancreatic cancer patients. The Tumor Immune Estimation Resource (TIMER) web was used to investigate the pertinence between NSG3 and immune cell infiltration.

Statistical analysis

The GraphPad Prism 7.0 software was employed to analyze statistical differences. The statistical significance was evaluated via Student's t-test and one or two-way analysis of variance (ANOVA). *P* values < 0.05 were considered statistically significant. The data were showed as the means ± SD.

Results

Decreased NSG3 expression in pancreatic cancer caused poor prognosis

To illustrate the role of NSG3 in PC, we used the GEPIA web tool to analyze the survival differences between low and high NSG3 expression levels. According to our results, patients with high NSG3 expression had better prognoses (**Figure 1A** and **1B**) in terms of overall survival (OS) (HR = 0.46, Log-rank P = 0.00023) and disease-free survival (DFS) (HR = 0.61, Log-rank P = 0.027). The Human Protein Atlas also showed higher five-year survival rates (38%) in high NSG3-expressing patients than in low NSG3-expressing patients (21%) (**Figure 1C**). Moreover, we found that NSG3 expression levels decreased in PC cells, compared with normal cells (**Figure 1D**). Immunohistochemical staining using tissue microarray and IHC scoring based on the above-mentioned protocol revealed that the staining intensity was significantly weaker in cancerous tissues, compared with para-carcinoma tissues, indicating that NSG3 protein expression was down-regulated in PC (**Figure 1E** and **1F**). Therefore, the decrease in NSG3 expression levels caused the poor prognosis in pancreatic cancer.

Overexpressed NSG3 inhibited proliferation and invasion of PC cells in vitro

To further clarify biological function of NSG3 in PC, we constructed pancreatic cancer cell lines that could exogenously express Flag-NSG3, and we used western blotting and RT-qPCR to ensure that the expression efficiency of exogenous NSG3 was sufficient (**Figure 2A** and **2B**). Through the clone formation assay (**Figure 2C**) and MTS assay (**Figure 2D**), we found that the multiplication capacity of PC cells (PANC-1, BxPC-3, SW1990) was markedly suppressed when NSG3 was overexpressed. On the other hand, results from the transwell test showed invasion capacities of PC cells were significantly reduced when NSG3 was overexpressed (**Figure 2E**). The *in vivo* xenograft tumor assay further yielded similar findings. Tumor growth was significantly inhibited when NSG3 was overexpressed and considerably enhanced when NSG3 was knocked down, harboring the largest tumor mass and demonstrating the fastest growth rate (**Figure 2F**). These results suggest that overexpressed NSG3 suppresses proliferation and invasion of PC cells.

Decreased NSG3 expression promoted proliferation and invasion of PC cells in vitro

Analogously, gene-specific small hairpin RNA (shNSG3) was used to knock down NSG3

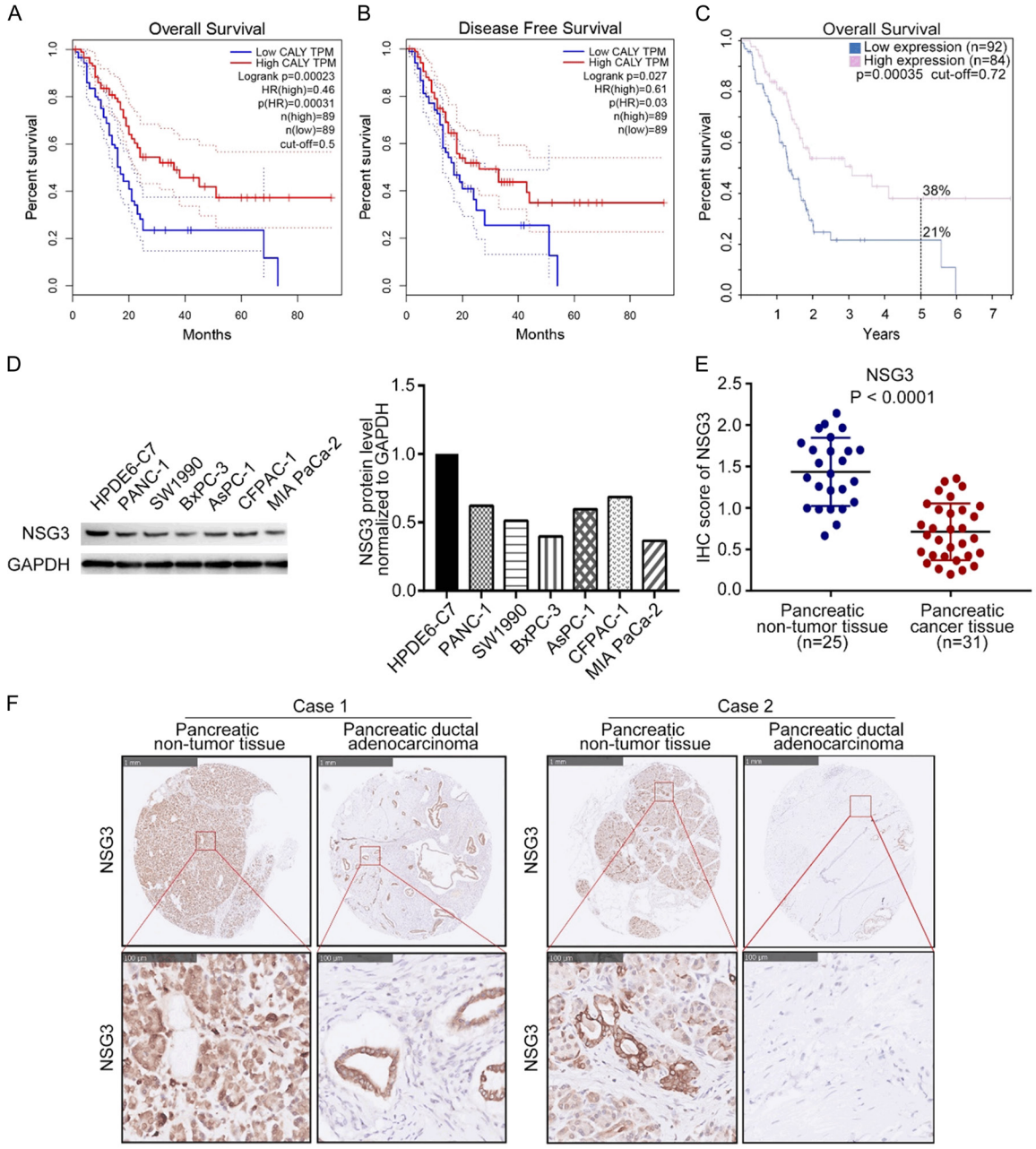

Figure 1. The decreased NSG3 expression caused poor prognosis in pancreatic cancer. (A and B) The GEPIA web tool was used to analyze the overall survival (A. HR = 0.46, Logrank P = 0.00023) and disease-free survival (B. HR = 0.61, Logrank P = 0.027) of pancreatic cancer patients. (C) The Human Protein Atlas database was searched to analyze the overall survival of pancreatic cancer patients (P = 0.00035). (D) The expression level of NSG3 was determined by Western blotting analysis in normal pancreatic ductal epithelial cells and pancreatic cancer cells from different sources. GAPDH was served as a loading control. (E) The expression level of NSG3 determined by IHC in pancreatic tissue microarray (pancreatic non-tumor tissue n = 25, pancreatic cancer n = 31), P < 0.0001. Student's t-test was used to test statistical differences. (F) The typical IHC image of NSG3 in pancreatic tissue microarray.

expression, and the knockdown efficiency was determined using western blotting and RT-qPCR (**Figure 3A** and **3B**). The clone formation assay (**Figure 3C**) and MTS assay (**Figure 3D**) revealed that pancreatic cancer cell reproductive capacity was enhanced significantly after NSG3 was knocked down. The invasion capability of pancreatic cancer cells was also

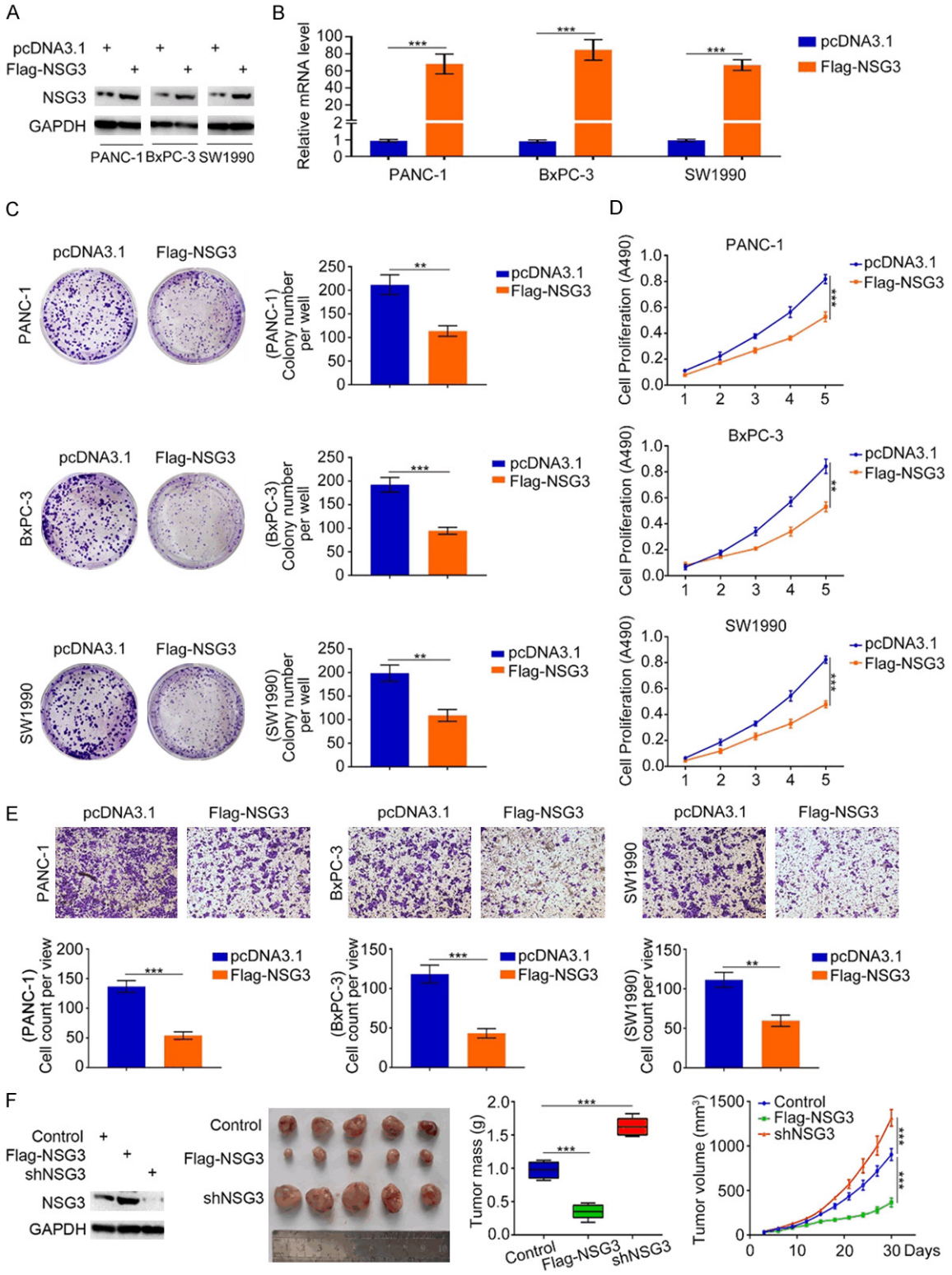

Figure 2. Overexpressed NSG3 inhibited proliferation and invasion of pancreatic cancer cells in vitro. (A and B) PANC-1, BxPC-3 and SW1990 cells were infected with pcDNA3.1 vector and Flag-NSG3 plasmid. After forty-eight hours postinfection, the cells were harvested for RT-qPCR analysis (B). And after seventy-two hours, the cells were harvested for Western blotting analysis (A). The data were shown as the mean values ± SD from three replicates. ***, $P < 0.001$. Student's t-test was used to test statistical differences. (C-E) PANC-1, BxPC-3 and SW1990 cells were infected with pcDNA3.1 vector and Flag-NSG3 plasmid. After 24 hours, cells were collected for clone formation (C), MTS assay (D) and transwell invasion (with matrigel) assay (E). All data were shown as the mean values ± SD

from three replicates. **, P < 0.01; ***, P < 0.001. Student's t-test was used to test statistical differences. Two-way ANOVA was used to test the statistical differences of cell proliferation. (F) PANC-1 cells were infected with indicated lentivirus. After 72 h, all cells were harvested for Western Blotting analysis. Then, cells were subcutanously injected into the nude mice. These tumors were harvested after 30 days for photograph, measurement and weight. Data presented as Means ± SD (n = 5). ***, P < 0.001. One-way ANOVA was used to test the statistical differences of tumor mass, and two-way ANOVA was used to test the statistical differences of tumor volume.

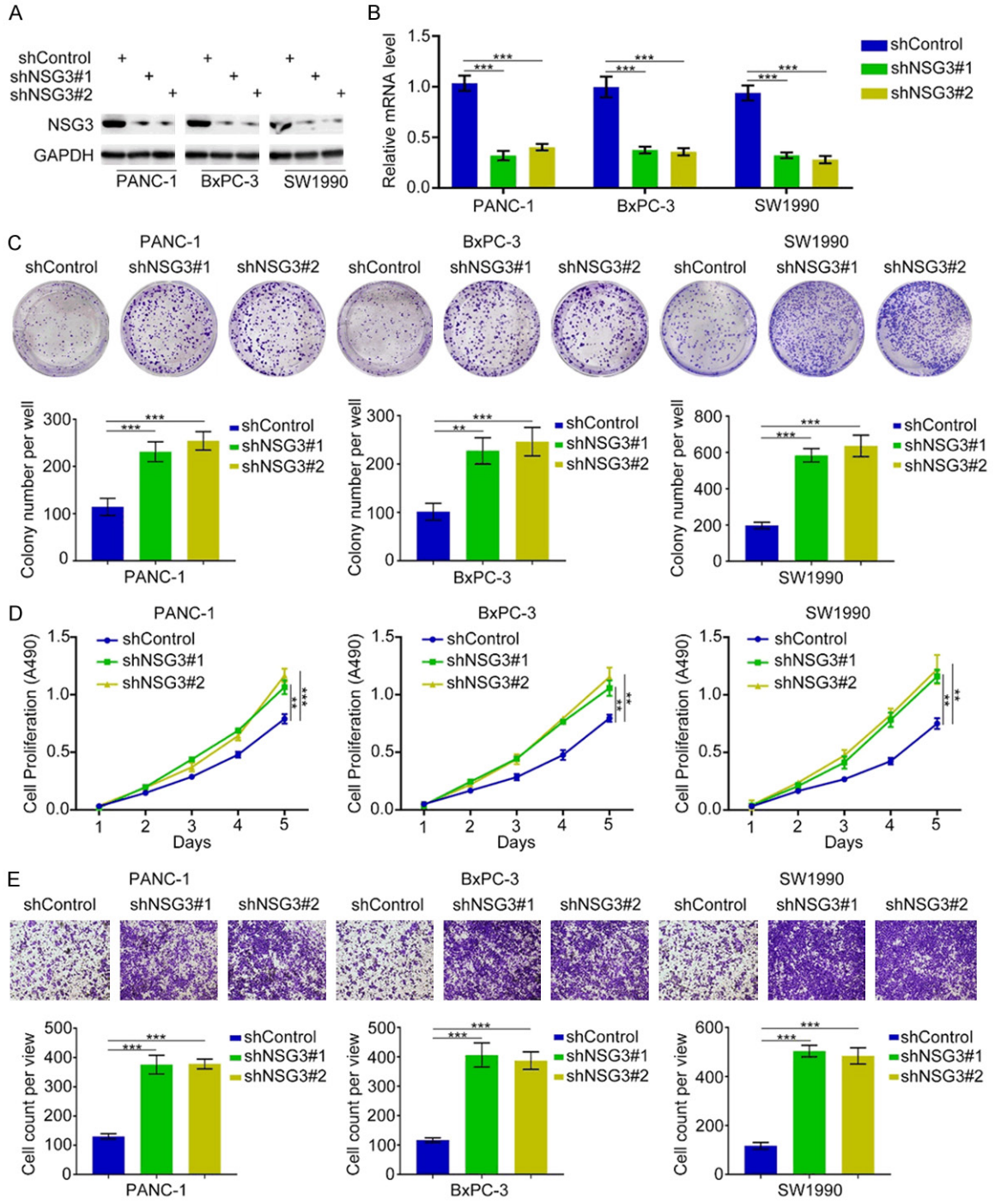

Figure 3. Knockout NSG3 promoted proliferation and invasion of pancreatic cancer cells in vitro. (A and B) PANC-1, BxPC-3 and SW1990 cells were infected with lentivirus vectors expressing control or NSG3-specific shRNAs. After forty-eight hours postinfection, the cells were harvested for RT-qPCR analysis (B). And after seventy-two hours, the cells were harvested for Western blotting analysis (A). The data were shown as the mean values ± SD from three

replicates. ***, P < 0.001. One-way ANOVA was used to test the statistical differences. (C-E) PANC-1, BxPC-3 and SW1990 cells were infected with lentivirus vectors expressing control or NSG3-specific shRNAs. After 24 hours, cells were collected for clone formation (C), MTS assay (D) and transwell invasion (with matrigel) assay (E). All data were shown as the mean values ± SD from three replicates. *, P < 0.05; **, P < 0.01; ***, P < 0.001. One-way ANOVA was used to test the statistical differences. Two-way ANOVA was used to test the statistical differences of cell proliferation.

strengthened in NSG3-knocked down PC cells (**Figure 3E**). The above results confirmed that knocking-down NSG3 promotes the malignant biological behaviors of PC cells.

Increased NSG3 inhibited PD-L1 expression in PC

Given that NSG3 suppressed the malignancy of pancreatic cancer, we further explored the specific molecular mechanisms of this process. Interestingly, we found an association between NSG3 expression and immune infiltration by CD4+ T cells and macrophage using the Tumor Immune Estimation Resource (TIMER) web analysis tool (**Figure 4A**). Therefore, we speculated that NSG3 might regulate the expression of immune checkpoint PD-L1. As anticipated, the expression of PD-L1 increased or decreased when NSG3 was knocked down or overexpressed, respectively, at both the transcription and translation levels (**Figure 4B** and **4C**). Besides, after overexpressing NSG3, we knocked down NSG3 again and found PD-L1 expression was significantly up-regulated again (**Figure 4D**). Moreover, the tissue microarray of pancreatic cancer (n = 31) was used to perform IHC analysis to illustrate the pertinence between NSG3 and PD-L1 in PC tissue (**Figure 4E**). The IHC scores of NSG3 and PD-L1 were obtained using the formula provided above and summarized on a heatmap (**Figure 4F**). After plotting the IHC scores of NSG3 and PD-L1 on a scatter diagram, we found that NSG3 and PD-L1 expressions in PC tissues correlated negatively (Spearman r = -0.5539, *P* = 0.0012) (**Figure 4G**). In a nutshell, NSG3 suppressed PD-L1 expression in PC.

NSG3 inhibited PD-L1 expression by suppressing Erk1/2 phosphorylation

To further figure out the potential regulatory mechanism of NSG3 on PD-L1, NSG3 was knocked down or overexpressed to perform western blotting to explore the possible changes in signaling pathways. We found that the phosphorylation level of Erk1/2 increased in the pancreatic cancer cells with knocked-down NSG3, but total Erk1/2 levels did not change (**Figure 5A**). Conversely, Erk1/2 phosphorylation level was down-regulated in PC cells overexpressing NSG3 (**Figure 5B**).

To verify whether the Erk1/2 signaling pathways mediated the regulation of PD-L1 by NSG3, we used AG126 (Erk1/2 inhibitor) to inhibit Erk1/2 phosphorylation after NSG3 expression was knocked down, and the result was a weakened up-regulated PD-L1 expression (**Figure 5C**). These findings indicate that NSG3 inhibited PD-L1 expression by suppressing the phosphorylation of Erk1/2 (**Figure 5D**).

NSG3 and the anti-PD-1 antibody immune checkpoint inhibitor acted synergistically, enhancing the efficacy of the inhibitor

Considering that NSG3 inhibited PD-L1 expression in this study, we speculated increased NSG3 expression in PC might improve the efficacy of anti-PD-1 antibody immune checkpoint inhibitors. First, we constructed a murine pancreatic cancer cell line (PANC02) that stably overexpressed NSG3 and evaluated the expression efficiency using western blotting and RT-qPCR (**Figure 6A** and **6B**). PANC02 cells were injected into the left-back of C57BL/6 mice subcutaneously until xenografts volume reached 50 mm^3. Mice were treated with intraperitoneal injection using a 200 ug anti-PD-1 antibody or IgG antibody on days 0, 3, and 6 (**Figure 6C**). Consistent with subcutaneous tumor formation in nude mice, the tumor growth rate in C57BL/6 mice reduced when NSG3 was overexpressed (**Figure 6D**). More importantly, tumor growth was slower in C57BL/6 mice that overexpressed NSG3 and were injected intraperitoneally with the anti-PD-1 antibody (**Figure 6D**). Additionally, the mice model with Flag-NSG3-treated PANC02 cells obtained a significantly longer survival time (**Figure 6E**).

After the natural death of the mice, the tumors were dissected for flow cytometry, with results showing that CD45+ CD4+ T cell and

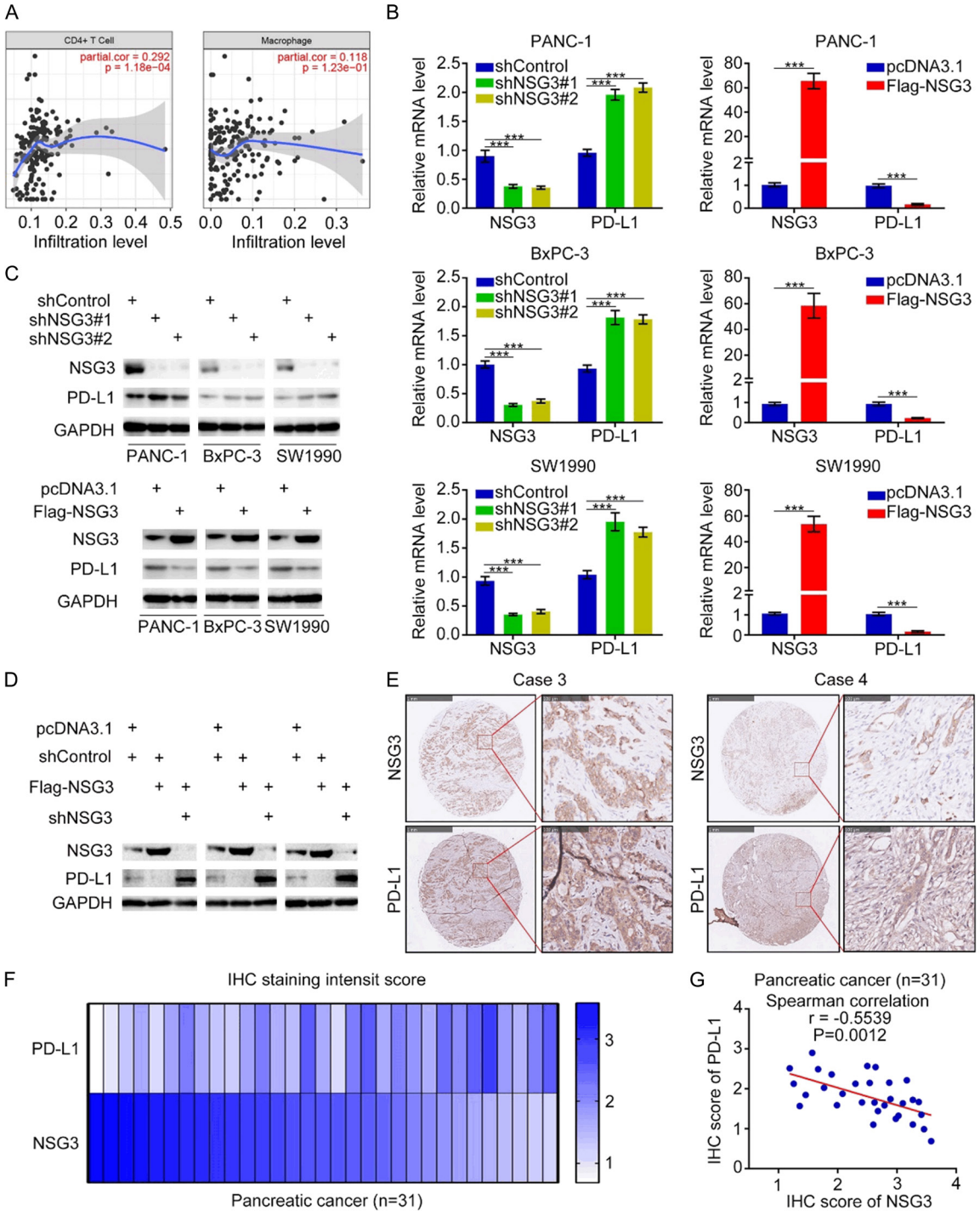

Figure 4. NSG3 inhibited the expression of PD-L1 in pancreatic cancer. (A) Tumor IMmune Estimation Resource (TIMER) web tool was used to analyze the relationship between NSG3 and immune infiltration (CD4+ T cell and macrophage). (B, C) PANC-1, BxPC-3 and SW1990 cells were infected with lentivirus vectors expressing control or NSG3-specific shRNAs. After forty-eight hours postinfection, the cells were harvested for RT-qPCR analysis (B). And after seventy-two hours, the cells were harvested for Western blotting analysis (C). The data were shown as the mean values ± SD from three replicates. ***, $P < 0.001$. One-way ANOVA was used to test the statistical differences. (D) PANC-1, BxPC-3 and SW1990 cells were infected with indicated plasmids (Flag-NSG3 and shNSG3). After infecting 72 h, all cells were collected for Western Blotting analysis. (E-G) The tissue microarray of pancreatic cancer (n = 31) was stained with NSG3 and PD-L1 respectively. The typical images of NSG3 and PD-L1 were displayed (E). NSG3 and PD-L1 IHC score of tissue microarray of pancreatic cancer was plotted the heatmap (F) and the scatter diagram (G). Student's t-test was used to test statistical differences.

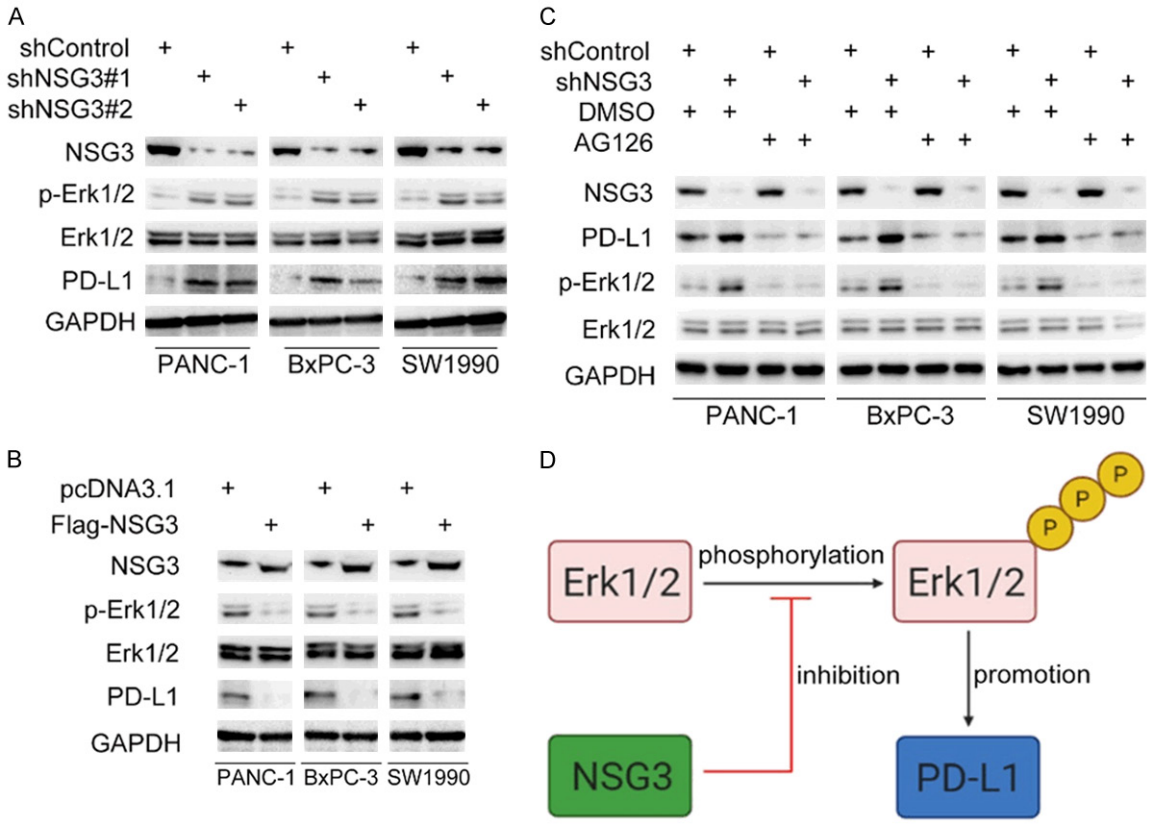

Figure 5. NSG3 inhibited PD-L1 expression by suppressing the phosphorylation of Erk1/2. A. PANC-1, BxPC-3 and SW1990 cells were infected with lentivirus vectors expressing control or NSG3-specific shRNAs. After 72 hours postinfection, the cells were harvested for Western blotting analysis. B. PANC-1, BxPC-3 and SW1990 cells were infected with pcDNA3.1 or Flag-NSG3 plasmid. After 72 hours postinfection, the cells were harvested for Western blotting analysis. C. PANC-1, BxPC-3 and SW1990 cells were infected with lentivirus vectors expressing control or NSG3-specific shRNAs. After 48 hours infection, the cells were treated with AG126 (25 uM) for another 24 hours. Then, cells were harvested for Western blotting analysis. D. NSG3 inhibited the phosphorylation level of ERK1/2 to regulate the expression of PD-L1.

CD45+CD8+ T cell infiltrations increased and CD11b+Gr1+ T cell infiltration decreased in NSG3-overexpressing cells (**Figure 6F**). Furthermore, there were more CD45+CD4+ T cell and CD45+CD8+ T cell infiltrations and fewer CD11b+Gr1+ T cell infiltration in tumor tissues overexpressing NSG3 and given an anti-PD-1 antibody (**Figure 6F**). These data indicate that overexpressed NSG3 could hold back immunosuppression by pancreatic cancer and act synergistically with anti-PD-1 antibody immune checkpoint inhibitors to enhance the curative effect of the inhibitors.

Discussion

As a new type of tumor treatment, immunotherapy, particularly anti-PD-1/PD-L1 monoclonal antibody, is seen as a promising approach. However, several clinical trials have highlighted the failure by immune checkpoint inhibition to cause efficacy and improve prognosis in patients with pancreatic cancer [18-21]. Combined treatment options, including chemotherapy, have shown preliminary promise, though [19, 22-25]. Therefore, it is necessary to explore a new combination treatment program that enhances the curative effect of anti-PD-1/PD-L1 monoclonal antibodies.

NSG3 is a calcyon neuron-specific vesicular protein that mediates the fluidity and storage characteristics of calcium-containing vesicles [26] and is closely linked to neuropsychiatric diseases, such as schizophrenia and Alzheimer disease [27]. Here, we revealed NSG3 antitumor effect and showed NSG3 expression level was down-regulated in PC, which suggests

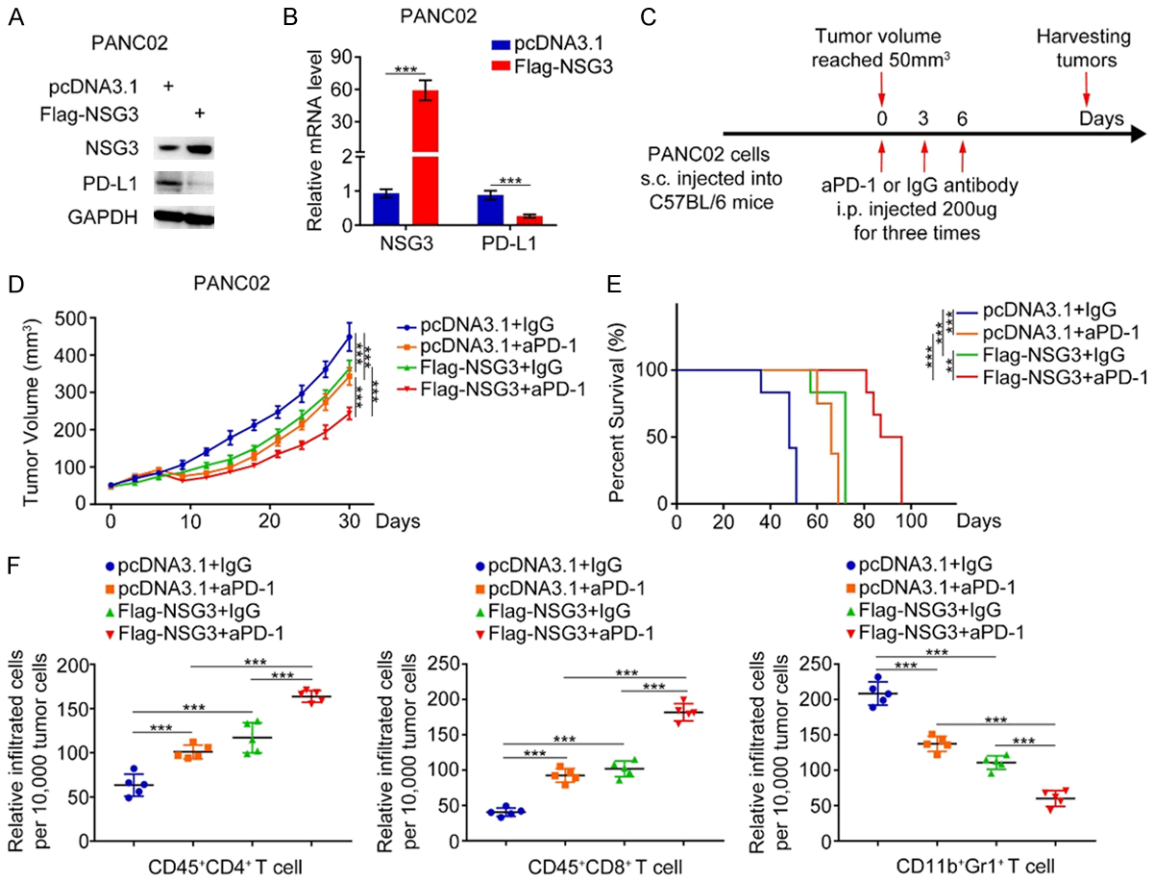

Figure 6. NSG3 synergistically enhanced the efficacy of immune checkpoint inhibitor anti-PD-1 antibody. (A and B) PANC02 cells were infected with lentivirus vectors expressing control or Flag-NSG3 lentivirus. The cells were harvested for Western blotting analysis (A) and RT-qPCR analysis (B). The data were shown as the mean values ± SD. ***, $P < 0.001$. Student's t-test was used to test statistical differences. (C) After 72 h of selection with puromycin, 5×10^6 PANC02 cells infected with pcDNA3.1 or Flag-NSG3 were subcutaneously injected into the left back of C57BL/6 mice. Mice with subcutaneous PANC02 tumors (n = 5/group) were treated with anti-PD-1 antibody (200 μg) or nonspecific IgG antibody for three times shown as the schematic diagram (C). (D) The growth curves of PANC02 tumors with the different treatments were shown in (D). The data were shown as the mean values ± SD (n = 5). ***, $P < 0.001$. Two-way ANOVA was used to test statistical differences. (E) Kaplan-Meier survival curves for each treatment group demonstrated the improved efficacy of combining anti-PD-1 antibody with NSG3 overexpression. **, $P < 0.01$; ***, $P < 0.001$ (Gehan-Breslow-Wilcoxo test). (F) After all mice died naturally, the PANC02 tumors was excised from the mice were dissociated, and tumor cells were harvested for Flow cytometry analysis to detect the numbers of tumor infiltrating lymphocyte (TILs). All data were shown as means ± SD (n = 5). ***, $P < 0.001$. One-way ANOVA was used to test statistical differences.

that NSG3 is associated with the development and progression of pancreatic tumors. Interestingly, our study is not the first to find that the expression level of NSG3 reduces in tumors. Potter N et al. found that NSG3 located on chromosome 10q26.3 exhibited the loss of individual clone in pediatric pilocytic astrocytoma, which was associated with reduced gene expression [17]. Regrettably, this study failed to explore the detailed mechanism of NSG3. Nonetheless, the biological function of NSG3 needs to be studied in more tumor types.

Immunosuppression and tumor immune escape are the major reasons pancreatic cancer immunotherapy fails. PD-1, a T cell inhibitory receptor, could interact with its ligand PD-L1 [28]. But under the pathological conditions of cancer, PD-L1 is frequently overexpressed abnormally in tumor cells, causing effective immunosuppression and tumor immune escape [29-32]. PD-1/PD-L1 blockade enhances anti-tumor immune effect via suppressing immunosuppressive pathway. Thus, an in-depth study for PD-L1 expression reason is of

great significance for blocking out PD-L1 process and would provide new immunotherapy strategies in pancreatic cancer. Recent investigations have revealed that the excessive activation of the Kras-Erk1/2 signaling pathway induces PD-L1 expression in lung cancer [33, 34]. Here, we discovered NSG3 inhibited Erk1/2 phosphorylation, thereby preventing their induction and the subsequent activation of PD-L1 expression in PC. This research suggests NSG3 boosts the anti-tumor efficiency of PD-1/PD-L1 inhibitors and could also act as an Erk1/2 inhibitor.

Our study also suggested that more CD45+ CD4+ T cells and CD45+CD8+ T cells were recruited by tumor tissues after overexpressing NSG3, whereas, CD11b+Gr1+ T cells infiltration with immunosuppressive ability decreased, causing tumor volume to shrink and prolonging survival in mice. As anticipated, administering an anti-PD-1 antibody to mice overexpressing NSG3 further boosts treatment. These data, therefore, provide a theoretical basis for future clinical applications.

Conclusion

In this research, we found that pancreatic cancer cells had diminished levels of NSG3 expression, which led to poor prognoses for pancreatic cancer patients. NSG3 expression also led to the suppression of proliferation, invasion, and migration in PC cells. We further established that NSG3 inhibited PD-L1 expression by suppressing Erk1/2 phosphorylation to improve the immune response to pancreatic cancer. Hence, NSG3 is a potential new diagnostic and prognostic marker, particularly useful in immune checkpoint blockade therapy.

Acknowledgements

Thanks to the Department of Pancreatic Surgery, Union Hospital, Tongji Medical College, Huazhong University of Science and Technology, for providing us with laboratory site.

Disclosure of conflict of interest

None.

Abbreviations

PC, Pancreatic cancer; NSG3 (CALY), Calcyon neuron specific vesicular protein; PD-1, Programmed death 1; PD-L1, Programmed death-ligand 1; OS, Overall survival; DFS, Disease free survival; IHC, Immunohistochemistry; GEPIA, Gene Expression Profiling Interaction Analysis; TIMER, Tumor IMmune Estimation Resource; MTS, 3-(4,5-dimethylthiazol-2-yl)-5-(3-carboxymethoxyphenyl)-2-(4-sulfophenyl)-2H-tetrazolium; TMA, Tissue microarray.

Address correspondence to: Feiyang Wang and Rui Wang, Sino-German Laboratory of Personalized Medicine for Pancreatic Cancer, Union Hospital, Tongji Medical College, Huazhong University of Science and Technology, Wuhan 430022, China. E-mail: 1335528702@qq.com (FYW); wangrui_217@sohu.com (RW)

References

[1] Ferlay J, Soerjomataram I, Dikshit R, Eser S, Mathers C, Rebelo M, Parkin DM, Forman D and Bray F. Cancer incidence and mortality worldwide: sources, methods and major patterns in GLOBOCAN 2012. Int J Cancer 2015; 136: E359-E386.

[2] Ansari D, Tingstedt B, Andersson B, Holmquist F, Sturesson C, Williamsson C, Sasor A, Borg D, Bauden M and Andersson R. Pancreatic cancer: yesterday, today and tomorrow. Future Oncol 2016; 12: 1929-1946.

[3] Siegel RL, Miller KD and Jemal A. Cancer statistics, 2018. CA Cancer J Clin 2018; 68: 7-30.

[4] Zhu H, Li T, Du Y and Li M. Pancreatic cancer: challenges and opportunities. BMC Med 2018; 16: 214.

[5] Grasso C, Jansen G and Giovannetti E. Drug resistance in pancreatic cancer: impact of altered energy metabolism. Crit Rev Oncol Hematol 2017; 114: 139-152.

[6] Casey SC, Tong L, Li Y, Do R, Walz S, Fitzgerald KN, Gouw AM, Baylot V, Gütgemann I, Eilers M and Felsher DW. MYC regulates the antitumor immune response through CD47 and PD-L1. Science 2016; 352: 227-231.

[7] Kuol N, Stojanovska L, Nurgali K and Apostolopoulos V. PD-1/PD-L1 in disease. Immunotherapy 2018; 10: 149-160.

[8] Sun Z, Fourcade J, Pagliano O, Chauvin JM, Sander C, Kirkwood JM and Zarour HM. IL10 and PD-1 cooperate to limit the activity of tumor-specific CD8+ T cells. Cancer Res 2015; 75: 1635-1644.

[9] Butte MJ, Keir ME, Phamduy TB, Sharpe AH and Freeman GJ. Programmed death-1 ligand 1 interacts specifically with the B7-1 costimulatory molecule to inhibit T cell responses. Immunity 2007; 27: 111-122.

[10] Alsaab HO, Sau S, Alzhrani R, Tatiparti K, Bhise K, Kashaw SK and Iyer AK. PD-1 and PD-L1

checkpoint signaling inhibition for cancer immunotherapy: mechanism, combinations, and clinical outcome. Front Pharmacol 2017; 8: 561.
[11] Francisco LM, Sage PT and Sharpe AH. The PD-1 pathway in tolerance and autoimmunity. Immunol Rev 2010; 236: 219-242.
[12] Muthusamy N, Faundez V and Bergson C. Calcyon, a mammalian specific NEEP21 family member, interacts with adaptor protein complex 3 (AP-3) and regulates targeting of AP-3 cargoes. J Neurochem 2012; 123: 60-72.
[13] Alberi S, Boda B, Steiner P, Nikonenko I, Hirling H and Muller D. The endosomal protein NEEP21 regulates AMPA receptor-mediated synaptic transmission and plasticity in the hippocampus. Mol Cell Neurosci 2005; 29: 313-319.
[14] Davidson HT, Xiao J, Dai R and Bergson C. Calcyon is necessary for activity-dependent AMPA receptor internalization and LTD in CA1 neurons of hippocampus. Eur J Neurosci 2009; 29: 42-54.
[15] Norstrom EM, Zhang C, Tanzi R and Sisodia SS. Identification of NEEP21 as a β-amyloid precursor protein-interacting protein in vivo that modulates amyloidogenic processing in vitro. J Neurosci 2010; 30: 15677-15685.
[16] Laurin N, Misener VL, Crosbie J, Ickowicz A, Pathare T, Roberts W, Malone M, Tannock R, Schachar R, Kennedy JL and Barr CL. Association of the calcyon gene (DRD1IP) with attention deficit/hyperactivity disorder. Mol Psychiatry 2005; 10: 1117-1125.
[17] Potter N, Karakoula A, Phipps KP, Harkness W, Hayward R, Thompson DNP, Jacques TS, Harding B, Thomas DGT, Palmer RW, Rees J, Darling J and Warr TJ. Genomic deletions correlate with underexpression of novel candidate genes at six loci in pediatric pilocytic astrocytoma. Neoplasia 2008; 10: 757-772.
[18] Feng M, Xiong G, Cao Z, Yang G, Zheng S, Song X, You L, Zheng L, Zhang T and Zhao Y. PD-1/PD-L1 and immunotherapy for pancreatic cancer. Cancer Lett 2017; 407: 57-65.
[19] Henriksen A, Dyhl-Polk A, Chen I and Nielsen D. Checkpoint inhibitors in pancreatic cancer. Cancer Treat Rev 2019; 78: 17-30.
[20] Brahmer JR, Tykodi SS, Chow LQM, Hwu WJ, Topalian SL, Hwu P, Drake CG, Camacho LH, Kauh J, Odunsi K, Pitot HC, Hamid O, Bhatia S, Martins R, Eaton K, Chen S, Salay TM, Alaparthy S, Grosso JF, Korman AJ, Parker SM, Agrawal S, Goldberg SM, Pardoll DM, Gupta A and Wigginton JM. Safety and activity of anti-PD-L1 antibody in patients with advanced cancer. N Engl J Med 2012; 366: 2455-2465.
[21] Royal RE, Levy C, Turner K, Mathur A, Hughes M, Kammula US, Sherry RM, Topalian SL, Yang JC, Lowy I and Rosenberg SA. Phase 2 trial of single agent Ipilimumab (anti-CTLA-4) for locally advanced or metastatic pancreatic adenocarcinoma. J Immunother 2010; 33: 828-33.
[22] Gao M, Lin M, Moffitt RA, Salazar MA, Park J, Vacirca J, Huang C, Shroyer KR, Choi M, Georgakis GV, Sasson AR, Talamini MA and Kim J. Direct therapeutic targeting of immune checkpoint PD-1 in pancreatic cancer. Br J Cancer 2019; 120: 88-96.
[23] Winograd R, Byrne KT, Evans RA, Odorizzi PM, Meyer ARL, Bajor DL, Clendenin C, Stanger BZ, Furth EE, Wherry EJ and Vonderheide RH. Induction of T-cell immunity overcomes complete resistance to PD-1 and CTLA-4 blockade and improves survival in pancreatic carcinoma. Cancer Immunol Res 2015; 3: 399-411.
[24] Weiss GJ, Waypa J, Blaydorn L, Coats J, McGahey K, Sangal A, Niu J, Lynch CA, Farley JH and Khemka V. A phase Ib study of pembrolizumab plus chemotherapy in patients with advanced cancer (PembroPlus). Cancer Immunol Res 2017; 117: 33-40.
[25] Mahalingam D, Wilkinson GA, Eng KH, Fields P, Raber P, Moseley JL, Cheetham K, Coffey M, Nuovo G, Kalinski P, Zhang B, Arora SP and Fountzilas C. Pembrolizumab in combination with the oncolytic virus pelareorep and chemotherapy in patients with advanced pancreatic adenocarcinoma: a phase ib study. Clin Cancer Res 2020; 26: 71-81.
[26] Kruusmägi M, Zelenin S, Brismar H and Scott L. Intracellular dynamics of calcyon, a neuron-specific vesicular protein. Neuroreport 2007; 18: 1547-1551.
[27] Muthusamy N, Chen YJ, Yin DM, Mei L and Bergson C. Complementary roles of the neuron-enriched endosomal proteins NEEP21 and calcyon in neuronal vesicle trafficking. J Neurochem 2015; 132: 20-31.
[28] Sun L, St Leger AJ, Yu CR, He C, Mahdi RM, Chan CC, Wang H, Morse HC and Egwuagu CE. Interferon regulator factor 8 (IRF8) limits ocular pathology during HSV-1 infection by restraining the activation and expansion of CD8+ T cells. PLoS One 2016; 11: e0155420.
[29] Munir S, Andersen GH, Met Ö, Donia M, Frøsig TM, Larsen SK, Klausen TW, Svane IM and Andersen MH. HLA-restricted CTL that are specific for the immune checkpoint ligand PD-L1 occur with high frequency in cancer patients. Cancer Res 2013; 73: 1764-1776.
[30] Hirano F, Kaneko K, Tamura H, Dong H, Wang S, Ichikawa M, Rietz C, Flies DB, Lau JS, Zhu G, Tamada K and Chen L. Blockade of B7-H1 and PD-1 by monoclonal antibodies potentiates cancer therapeutic immunity. Cancer Res 2005; 65: 1089-1096.

[31] Peng J, Hamanishi J, Matsumura N, Abiko K, Murat K, Baba T, Yamaguchi K, Horikawa N, Hosoe Y, Murphy SK, Konishi I and Mandai M. Chemotherapy induces programmed cell death-ligand 1 overexpression via the nuclear factor-κB to foster an immunosuppressive tumor microenvironment in ovarian cancer. Cancer Res 2015; 75: 5034-5045.

[32] Norde WJ, Maas F, Hobo W, Korman A, Quigley M, Kester MG, Hebeda K, Falkenburg JH, Schaap N, de Witte TM, van der Voort R and Dolstra H. PD-1/PD-L1 interactions contribute to functional T-cell impairment in patients who relapse with cancer after allogeneic stem cell transplantation. Cancer Res 2011; 71: 5111-5122.

[33] Chen N, Fang W, Lin Z, Peng P, Wang J, Zhan J, Hong S, Huang J, Liu L, Sheng J, Zhou T, Chen Y, Zhang H and Zhang L. KRAS mutation-induced upregulation of PD-L1 mediates immune escape in human lung adenocarcinoma. Cancer Immunol Immunother 2017; 66: 1175-1187.

[34] Jiang L, Guo F, Liu X, Li X, Qin Q, Shu P, Li Y and Wang Y. Continuous targeted kinase inhibitors treatment induces upregulation of PD-L1 in resistant NSCLC. Sci Rep 2019; 9: 3705.

Table S1. The sequences of gene-specific shRNAs

shNSG3#1	CCGGACGGATGATCGCCTTCGCCATCTCGAGATGGCGAAGGCGATCATCCGTTTTTTTG
shNSG3#2	CCGGACAAGATCTGCACGCCGCTGACTCGAGTCAGCGGCGTGCAGATCTTGTTTTTTTG

Table S2. The sequences of RT-qPCR primers

Gene	Forward primer (5'-3')	Reverse primer (5'-3')
NSG3 (Human)	ATCCACATCCGCATCGTC	TACAGGGGAAAGCTGTATTTTAA
NSG3 (Mouse)	GTAGGGGTTGAGAGTCTATGTGG	CCAGATAGATGTGAATCTTTACTTAA
PD-L1 (Human)	GGACAAGCAGTGACCATCAAG	CCCAGAATTACCAAGTGAGTCCT
PD-L1 (Mouse)	GCTCCAAAGGACTTGTACGTG	TGATCTGAAGGGCAGCATTTC
GAPDH (Human)	ACCCACTCCTCCACCTTTGAC	TGTTGCTGTAGCCAAATTCGTT
GAPDH (Mouse)	AGGTCGGTGTGAACGGATTTG	GGGGTCGTTGATGGCAACA